

Switching photochromic molecules adsorbed on optical microfibres

U. Wiedemann, W. Alt, and D. Meschede*

Institut für Angewandte Physik, Universität Bonn, Wegelerstr. 8, 53115 Bonn, Germany

[*meschede@iap.uni-bonn.de](mailto:meschede@iap.uni-bonn.de)

Abstract: The internal state of organic photochromic spiropyran molecules adsorbed on optical microfibres is optically controlled and measured by state-dependent light absorption. Repeated switching between the states is achieved by exposure to the evanescent field of a few nanowatts of light guided in the microfibre. By adjusting the microfibre evanescent field strength the dynamic equilibrium state of the molecules is controlled. Time-resolved photoswitching dynamics are measured and modelled with a rate equation model. We also study how many times the photochromic system can be switched before undergoing significant photochemical degradation.

© 2012 Optical Society of America

OCIS codes: (060.2370) Fiber optics sensors; (160.5335) Photosensitive materials; (260.5130) Photochemistry; (300.6390) Spectroscopy, molecular.

References and links

1. L. Tong, R. R. Gattass, J. B. Ashcom, S. He, J. Lou, M. Shen, I. Maxwell, and E. Mazur, "Subwavelength-diameter silica wires for low-loss optical wave guiding," *Nature* **426**, 816–819 (2003).
2. G. Brambilla, F. Xu, P. Horak, Y. Jung, F. Koizumi, N. P. Sessions, E. Koukharenko, X. Feng, G. S. Murugan, and J. S. Wilkinson, "Optical fiber nanowires and microwires: fabrication and applications," *Adv. Opt. Photon.* **1**, 107–161 (2009).
3. G. Brambilla, "Optical fibre nanowires and microwires: a review," *J. Opt.* **12**, 043001 (2010).
4. U. Wiedemann, K. Karapetyan, C. Dan, D. Pritzkau, W. Alt, S. Irsen, and D. Meschede, "Measurement of sub-micrometre diameters of tapered optical fibres using harmonic generation," *Opt. Express* **18**, 7693–7704 (2010).
5. L. Tong and M. Sumetsky, *Subwavelength and nanometer diameter optical fibers* (Springer, Berlin, 2010).
6. G. Brambilla, V. Finazzi, and D. J. Richardson, "Ultra-low-loss optical fiber nanotapers," *Opt. Express* **12**, 2258–2263 (2004).
7. S. Leon-Saval, T. Birks, W. Wadsworth, P. St. J. Russell, and M. Mason, "Supercontinuum generation in submicron fibre waveguides," *Opt. Express* **12**, 2864–2869 (2004).
8. J. Ward, D. O'Shea, B. J. Shortt, M. J. Morrissey, K. Deasy, and S. N. Chormaic, "Heat-and-pull rig for fiber taper fabrication," *Rev. Sci. Instrum.* **77**, 083105 (2006).
9. F. Warken, A. Rauschenbeutel, and T. Bartholomäus, "Fiber pulling profits from precise positioning," *Photon. Spectra* **42**, 3, 73 (2008).
10. L. Tong, J. Lou, and E. Mazur, "Single-mode guiding properties of subwavelength-diameter silica and silicon wire waveguides," *Opt. Express* **12**, 1025–1035 (2004).
11. R. Garcia-Fernandez, W. Alt, F. Bruse, C. Dan, K. Karapetyan, O. Rehband, A. Stiebeiner, U. Wiedemann, D. Meschede, and A. Rauschenbeutel, "Optical nanofibers and spectroscopy," *Appl. Phys. B* **105**, 3–15 (2011).
12. F. Warken, E. Vetsch, D. Meschede, M. Sokolowski, and A. Rauschenbeutel, "Ultra-sensitive surface absorption spectroscopy using sub-wavelength diameter optical fibers," *Opt. Express* **15**, 11952–11958 (2007).
13. H. Dürr and H. Bouas-Laurent, *Photochromism: molecules and systems* (Elsevier, Amsterdam, 2003).
14. M. Irie and K. Sayo, "Solvent effects on the photochromic reactions of diarylethene derivatives," *J. Phys. Chem.* **96**, 7671–7674 (1992).
15. K. Uchida, Y. Kido, T. Yamaguchi, and M. Irie, "Thermally irreversible photochromic systems. Reversible photocyclization of 2-(1-Benzothiophen-3-yl)-3-(2 or 3-thienyl)maleimide derivatives," *B. Chem. Soc. Jpn.* **71**, 1101–1108 (1998).

16. L. Raboin, M. Matheron, J. Biteau, T. Gacoin, and J. Boilot, "Photochromism of spirooxazines in mesoporous organosilica films," *J. Mater. Chem.* **18**, 3242–3248 (2008).
17. K. Kinashi, Y. Harada, and Y. Ueda, "Thermal stability of merocyanine form in spiropyran/silica composite film," *Thin Solid Films* **516**, 2532–2536 (2008).
18. T. Yoshida, A. Morinaka, and N. Funakoshi, "Photochromism of a vacuum-deposited 1',3',3'-trimethyl-6-hydroxyspiro[2H-1-benzopyran-2,2'-indoline] film," *J. Chem. Soc. Chem. Commun.* **1986**, 437–438 (1986).
19. R. A. Evans, T. L. Hanley, M. A. Skidmore, T. P. Davis, G. K. Such, L. H. Yee, G. E. Ball, and D. A. Lewis, "The generic enhancement of photochromic dye switching speeds in a rigid polymer matrix," *Nat. Mater.* **4**, 249–253 (2005).
20. M. Q. Zhu, L. Zhu, J. J. Han, W. Wu, J. K. Hurst, and A. D. Q. Li, "Spiropyran-based photochromic polymer nanoparticles with optically switchable luminescence," *J. Am. Chem. Soc.* **128**, 4303–4309 (2006).
21. G. Berkovic, V. Krongauz, and V. Weiss, "Spiropyrans and spirooxazines for memories and switches," *Chem. Rev.* **100**, 1741–1754 (2000).
22. M. Irie, "Diarylethenes for memories and switches," *Chem. Rev.* **100**, 1685–1716 (2000).
23. J. S. Harper, C. P. Botham, and S. Hornung, "Tapers in single-mode optical fibre by controlled core diffusion," *Electron. Lett.* **24**, 245–246 (1988).
24. K. Kinashi, S. Nakamura, Y. Ono, K. Ishida, and Y. Ueda, "Reverse photochromism of spiropyran in silica," *J. Photochem. Photobiol. A* **213**, 136–140 (2010).
25. E. Mohn, "Kinetic characteristics of a solid photochromic film," *Appl. Opt.* **2**, 1570–1576 (1973).
26. G. H. Brown, *Photochromism* (John Wiley & Sons, New York, 1971).
27. V. Malatesta, M. Milosa, R. Millini, L. Lanzini, P. Bortolus, and S. Monti, "Oxidative-degradation of organic photochromes," *Mol. Cryst. Liq. Cryst.* **246**, 303–310 (1994).
28. V. Malatesta, *Organic photochromic and thermochromic compounds 2: Physicochemical studies, biological applications, and thermochromism* (Kluwer Academic Press, 1999), Chap. 2.

1. Introduction

Tapered optical fibres with diameters on the order of one micrometre – optical microfibres (OMFs) – are a versatile tool for optical applications [1–5]. OMFs are produced from standard, commercially available optical fibres by the flame-brushing technique [6–9]. The large refractive index step at the cladding-air interface in an OMF results in tight confinement of the propagating mode [10]. Thus, the light intensity is very high – not only inside the fibre but also in its evanescent field. At the same time the light remains confined along the fibre waist over a length of up to several centimetres. These properties make OMFs an excellent device for light-matter interaction experiments with the fibre environment [5, 11], for example with surface-adsorbates, vapours, and liquids.

In previous experiments we have demonstrated ultra-sensitive absorption spectroscopy of organic dye molecules adsorbed on OMFs [12]. After the passive observation of organic dyes, the next level of complexity is the optical switching of molecules. Candidates for active optical switching are organic photochromic molecules. The combination of functional optical molecules with fibre-based devices seems ideally suited for applications including photochromic fibre Bragg gratings and optical fibre switches as well as for studying prospective surface-adsorbed molecules for data storage.

Photochromism is defined as a reversible light-induced change of the absorption spectrum [13]. In typical photochromic systems only one molecular state exhibits a strong absorption band in the visible wavelength range and is therefore called the coloured state, the other state is called transparent. Both states absorb light in the UV wavelength range. Photochromism often comes along with a change in the physical and chemical properties and therefore provides many opportunities for research and applications. Experiments with photochromic molecules are usually performed in solution [14, 15], with photochromic films prepared by spin-coating [16, 17] or vacuum evaporation [18], and with photochromic molecules embedded in a polymer matrix [19, 20]. The basic potential of organic photochromic molecules for applications such as optical switches and data storage has been discussed by Berkovic et al. [21] and Irie [22].

The combination of OMFs with surface-adsorbed photochromic molecules is a system

providing strong light-matter coupling and convenient optical access to the internal states of the molecules by the fibre. We have prepared, detected and manipulated photochromic molecules adsorbed on OMFs. Measurements of the light-induced switching dynamics of surface-adsorbed photochromic molecules are modelled in a rough approximation using a rate equation model. With this simple model we are able to extract the relevant parameters of the system in a clear and intuitive way.

2. Switching surface-adsorbed photochromic organic molecules

We have used the commercially available fluorescent spiropyran *1-(2-Hydroxyethyl)-3,3-dimethylindolino-6'-nitrobenzopyrylospiran* which we will call "spiroOH". Photoswitching from the transparent to the coloured state occurs by exposure to UV light ("photocolouration") and the reverse photoswitching by exposure to white light ("photobleaching"). In solution, the coloured state relaxes thermally back to the transparent state, while in a silica matrix both states of spiroOH are thermally stable at room temperature [17]. Using OMFs we observed that both states of spiroOH adsorbed on silica are thermally stable as well.

2.1. Deposition of molecules

To deposit the molecules on OMFs a solution of 10 mg spiroOH in 50 ml toluene was prepared and then applied by the drip method [11]. The sublimation method [12] couldn't be used because spiroOH, as other common photochromic molecules, undergoes thermal decomposition before evaporating noticeably at atmospheric pressure. We have found that the polarity of the solvent strongly influences the number of molecules deposited on the fibre surface. Less polar solvents (heptane, toluene) leave many more molecules on the fibre compared to polar solvents (acetone, ethanol) for the same initial concentration of molecules. Moreover, by dripping a polar solvent onto the OMFs we are able to remove the surface-adsorbed molecules and reuse the fibre sample.

The surface-adsorbed organic molecules are detected using ultra-sensitive absorption spectroscopy with a sensitivity of better than 1 % of a monolayer [12]. We have not investigated whether the deposition from solution yields dilute layers of isolated molecules, such as the sublimation method [12], or rather islands, clusters or nanocrystals.

2.2. Experimental setup for detection and optical switching

In order to transmit UV light through the fibre sample, a special doubly-spliced fibre was fabricated: A UV-guiding fibre using fluorine-doped cladding (Nufern S630-HP, 3.5 μm core, 125 μm cladding, 590 ± 30 nm cutoff wavelength, NA = 0.12) was used to guide the UV and visible light to the fibre taper. Since fluorine-doped fibres lose the light guiding capability during pulling, which might be explained by the high diffusion rate of fluorine [23] resulting in a reduced refractive-index step, they cannot be used for tapering. In contrast, germanium-doped fibres are chemically stable under flame pulling, but slightly absorb UV light. Therefore a germanium-doped core single-mode fibre (Fibercore SM800, 4 μm core, 125 μm cladding, 730 ± 70 nm cutoff wavelength, NA = 0.12) was used to fabricate the taper and waist to adiabatically transfer the guided modes through the taper into the microfibre waist. The fibre sample used in all photoswitching experiments has a waist diameter of 0.42 μm and a waist length of 5 mm.

Figure 1 shows the experimental setup of the photoswitching experiment. White light from a fibre-coupled halogen lamp (Avantes AvaLight-HAL) is filtered by a 435 nm longpass filter to exclude UV or blue wavelength components and is coupled into the fibre sample. The molecules are continuously exposed to the white light during all measurements, thus they tend to be in the transparent state. The out coupled white light passes a dichroic mirror and is detected either

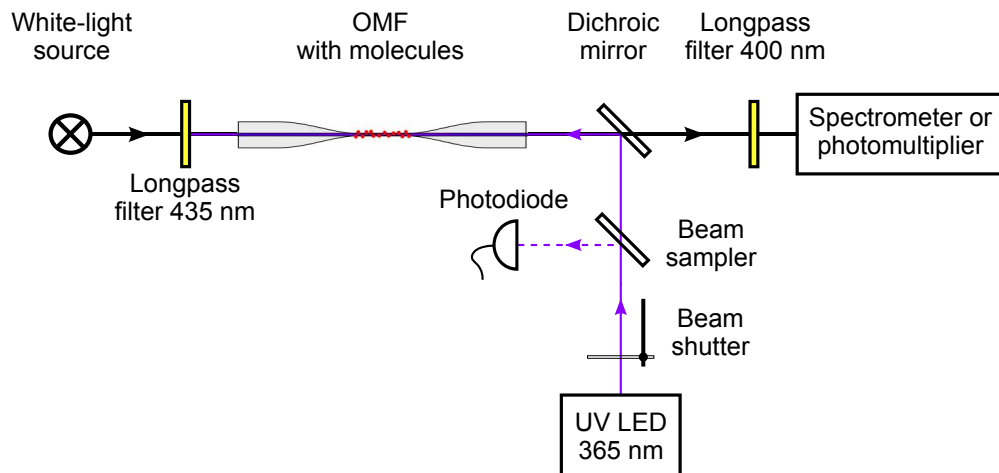


Fig. 1. Setup of the absorption spectroscopy and photoswitching experiment.

with a spectrometer (Avantes AvaSpec-ULS2048x16) or with a photomultiplier (Hamamatsu H5784).

Switching to the coloured state is induced by a UV LED at (365 ± 5) nm (Mightex FCS-0365-000) coupled into the fibre sample by reflection off the dichroic mirror. The UV exposure is controlled by a computer-driven beam shutter (Thorlabs SH05) and monitored by a photodiode. A 400 nm longpass filter installed in front of the detection device prevents UV light to enter the spectrometer or photomultiplier (PMT).

2.3. Absorbance spectrum

The present deposition procedure of photochromic molecules causes a spectrally broad background absorbance which might be explained by contaminations of the molecule solution. The spectral absorbance of the switchable coloured molecules in the visible wavelength range is determined by measuring the transmitted spectral power with all active molecules in the transparent state ($P_{\text{ref}}(\lambda)$) and the actual transmitted spectral power during and after photocoloration ($P_{\text{sig}}(\lambda)$). The white-light absorbance $A(\lambda)$ inferred from fibre-based surface absorption spectroscopy [12] is proportional to the number of coloured molecules N_{col} , making an excellent quantity to monitor photochromic processes:

$$A(\lambda) = -\log_{10} \frac{P_{\text{sig}}(\lambda)}{P_{\text{ref}}(\lambda)} \propto N_{\text{col}}. \quad (1)$$

The absorbance spectrum of spiroOH adsorbed on the OMF during the exposure to white light and UV and subsequently to white light only, i.e. during one cycle, is illustrated in Fig. 2(a) and 2(b), respectively. After 23 s the absorbance has almost decreased to zero suggesting that the switching cycle is nearly reversible. The measured absorbance spectrum of the coloured state is similar to measurements obtained with spiroOH dissolved in methanol [24].

2.4. Time-resolved absorbance

The temporal behaviour of the photoswitching process was studied using the spectrally integrated white-light transmission monitored with the PMT. From the PMT signal we calculate the integrated white-light absorbance A_{int} . Because of the spectrally inhomogeneous molecule

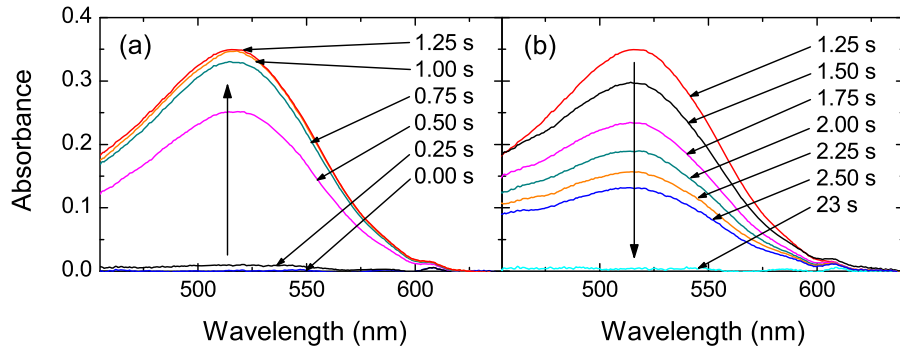


Fig. 2. (a) Absorbance spectra of spiroOH with continuous observation using 10 nW of white light and additional UV-light exposure (1.5 nW) starting in the time interval from 0 s to 0.25 s. With all molecules initially in the transparent state (blue curve), the absorbance increases by UV light up to a stable absorbance in the photostationary state (red curve). (b) Starting from the photostationary spectrum (red curve, $t = 1.25$ s) the absorbance decreases after the UV exposure has stopped. All curves obtained during UV exposure are slightly distorted due to broadband UV-induced fluorescence coming from the fibre. The integration time per spectrum is for all figures 250 ms.

absorbance the proportionality between the number of coloured molecules and A_{int} is not fulfilled. By averaging the molecule absorbance weighted with the wavelength-dependent PMT response and the inhomogeneous white-light spectrum we obtain a correction function. This function connects A_{int} with the peak absorbance of the molecule spectrum $A(\lambda_{\text{peak}})$ and thus restores the proportionality to N_{col} .

We observed even without molecules that the UV light causes an additional fluorescence signal originating from the fibre. Thus, the PMT signal is increased by a constant value during the UV exposure which was subtracted from the PMT signal. Small artefacts remaining when the shutter closes (see for example Fig. 3 at $t = 250$ ms) do not alter our analysis.

Figure 3 illustrates the absorbance dynamics (dots) during one switching cycle. The solid line shows the UV-light exposure. Although the UV-light power is below the white-light power, photocoloration is much faster than photobleaching.

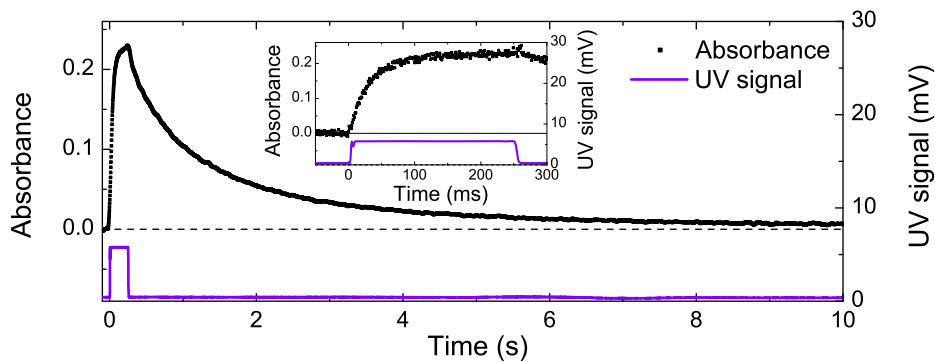


Fig. 3. Photoswitching dynamics of molecular absorbance (dots) for 250 ms exposure to 3 nW of UV light (solid line) and 10 nW of continuous white light. Dashed black line: zero absorbance. The graph was smoothed for visibility and the inset shows the horizontally expanded photocoloration process.

3. Rate equation model

The three main light-induced processes are photocoloration, photobleaching, and photodestruction (see Sect. 4). To gain further insight into the dynamic behaviour of the system we justify a simple mathematical model which allows us to estimate the relative switching rates.

3.1. Reaction dynamics: Photobleaching

In a general rate equation model of the photoswitching processes the reaction dynamics is governed by two nonlinear coupled differential equations depending on the position x along the fibre waist and the time t [25]. In a simplified model the position-dependence can be eliminated by introducing ensemble parameters, i.e. the total number of coloured molecules $N_{\text{col}}(t)$ and the total number of absorbed photons per second $J_{\text{col}}(t)$. Under this assumption we obtain for the rate equation of the photobleaching process

$$\frac{dN_{\text{col}}(t)}{dt} = -\Phi_{\text{photobleach}} \cdot J_{\text{col}}(t) \quad (2)$$

where $\Phi_{\text{photobleach}}$ is the quantum yield of the photobleaching process. Expressing N_{col} by the absorbance A and J_{col} by the fraction of absorbed photons calculated from the absorbance we obtain the nonlinear rate equation

$$\frac{dA(t)}{dt} = -a \cdot \Phi_{\text{photobleach}} \cdot (1 - 10^{-A(t)}). \quad (3)$$

Equation (3) can be used to numerically fit the measured absorbance using a as the fit parameter. In the weak absorption limit ($A \ll 1$) the last term in Eq. (3) can be approximated with $1 - 10^{-A} \approx \ln(10) \cdot A$ and thus becomes linear in A . The solution of the resulting linear rate equation

$$\frac{dA(t)}{dt} = -k \cdot A(t) \quad (4)$$

is an exponential function $A_0 \cdot \exp(-kt)$, where k is the rate constant. A weak absorption measurement is shown in Fig. 4. The data is only approximately described by an exponential function (red line). A much better fit is obtained by a bi-exponential decay (green line) indicating that the light-molecule coupling distribution is inhomogeneous. This inhomogeneous

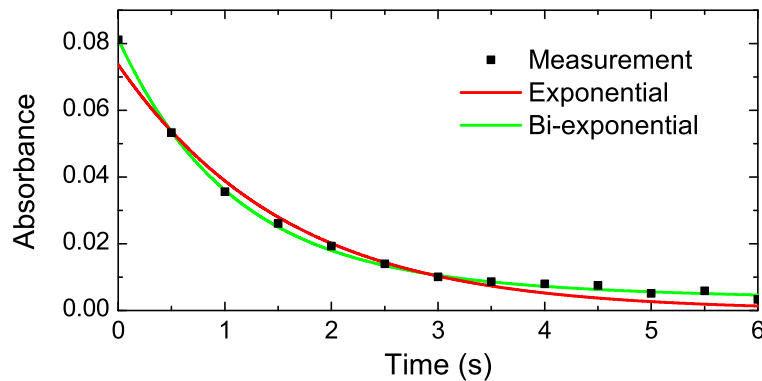


Fig. 4. Absorbance of spiroOH during photobleaching with white light. The solid lines represent the fit result obtained according to the exponential (red) and bi-exponential (green) model.

coupling can be explained for example by light absorption along the fibre, multi-mode light propagation, inhomogeneous local molecule adsorption sites, and molecules located not only on the waist, but also on the taper. Despite the limitation of the exponential model, it is a reasonable approximation to extract basic information about the relative switching rates. For the further quantitative analysis we therefore neglect the inhomogeneous light-molecule coupling and use the exponential model.

3.2. Photostationary states: Rates and coloured fraction

Exposing the molecules simultaneously to UV and white light leads to a dynamic equilibrium state (photostationary state). In the photostationary state the number of coloured molecules, and therefore the absorbance, does not change. The fraction of coloured molecules depends on the absorption cross section and the quantum yield of the molecules in both states, as well as on the irradiating light intensities. Therefore we can use the UV and white-light power to control the absorbance A_{stat} in the photostationary state. For the equilibrium state ($dA_{\text{stat}}/dt = 0$) the exponential rate equation model yields

$$A_{\text{stat}} = A_{\text{col}} \cdot \frac{k_{\text{photocol}}/k_{\text{photobleach}}}{1 + k_{\text{photocol}}/k_{\text{photobleach}}} \quad (5)$$

where A_{col} is the maximum absorbance if all switchable molecules are in the coloured state, k_{photocol} is the photocoloration rate proportional to the UV power and $k_{\text{photobleach}}$ is the photobleaching rate proportional to the white-light power. Enhancing the UV power by a UV power enhancement factor f_{enh} leads to a modified photocoloration rate and thus Eq. 5 transforms to

$$A_{\text{stat}}(f_{\text{enh}}) = A_{\text{col}} \cdot \frac{f_{\text{enh}} \cdot k_{\text{photocol},0}/k_{\text{photobleach},0}}{1 + f_{\text{enh}} \cdot k_{\text{photocol},0}/k_{\text{photobleach},0}} \quad (6)$$

where $k_{\text{photocol},0}$ and $k_{\text{photobleach},0}$ are the initial switching rates. The ratio of the switching rates can be thus obtained by varying the UV power and fitting the measured photostationary absorbance with this model.

Due to parasitic photodestruction the number of switchable molecules decreases after each cycle (see Sect. 4). To obtain a simple (approximately linear) form of the resulting decrease we keep the UV energy to which the molecules are exposed during one cycle constant. Thus we provide a constant fraction of destroyed molecules during each cycle. Figure 5(a) shows how to take into account the parasitic photodestruction of molecules over the course of the measurement by including a linear absorbance decrease to the fit function. From this measurement we find that the photocoloration rate k_{photocol} for 1.5 nW of UV light coupled into the OMF is 6.3 ± 1.7 times higher than the photobleaching rate $k_{\text{photobleach}}$ due to the 10 nW of white light. The error was calculated from four different measurements showing systematic deviations. These deviations might be explained by the photodestruction not allowing us to fully reach the photostationary state in every cycle. The UV-power dependent fraction of coloured molecules in the photostationary state is illustrated in Fig. 5(b). We are thus able to switch more than 95 % of the active molecules to the coloured state.

4. Photodestruction

The switching process itself is non-destructive, but light-induced parasitic side reactions lead to non-switchable by-products (photoproducts), which is also called fatigue [13]. We have therefore measured how often our photochromic system can be switched and quantified the fatigue characteristics of the spiroOH molecules.

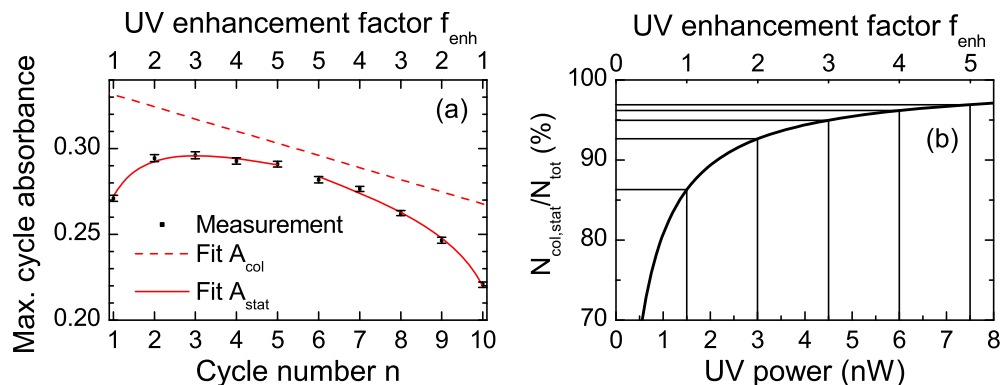


Fig. 5. (a) Absorbance in the photostationary state for 10 cycles with varying UV power, [1.5, 3, 4.5, 6, 7.5] nW and backwards. The exposure time of each cycle was varied inversely to the power to keep the UV energy to which the molecules are exposed in each cycle constant. Therefore in each cycle the same fraction of molecules is destroyed which allows us to discriminate between the molecule destruction and the saturation in the photostationary state (see text for details). The error bars show the statistical error and the solid lines are the fit curves according to Eq. 6 taking photodestruction (dashed line) into account. (b) Fraction of coloured molecules in the photostationary state depending on the UV-light power. The straight lines illustrate the specific UV powers used in the experiment and the corresponding fraction of coloured molecules.

4.1. Cyclability

A frequently used parameter to quantify how often a photochromic system can be switched is the cyclability Z_{50} . It is defined as the number of cycles to reduce the initial absorbance at a specific wavelength by 50 % [13], i.e. until half of the molecules are destroyed. The cyclability of a photochromic system is an important parameter to characterize the practicability of photochromic applications.

To characterize the repeatability of the photoswitching process we measured many subsequent switching cycles with spiroOH, see Fig. 6. During the photocoloration there is a cer-

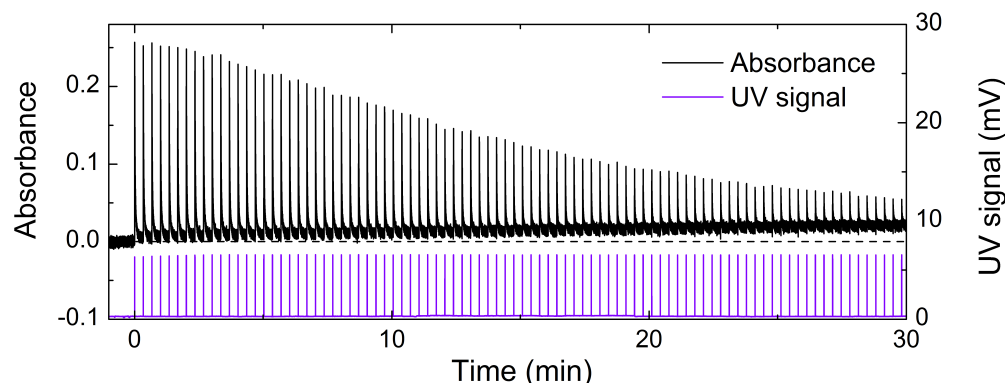


Fig. 6. Many subsequent switching cycles of spiroOH. Each cycle consists of 100 ms photocoloration (3 nW of UV) followed by 20 s photobleaching (10 nW of white light). The upper trace denotes the molecule absorbance, the lower trace the UV exposure, and the dashed black line zero absorbance.

tain probability for UV-induced photodestruction processes. Therefore the maximum peak absorbance decreases with the number of switching cycles due to the reduced amount of switchable molecules. The non-exponential decrease at the beginning again underlines the inhomogeneous light-molecule coupling. Moreover, the minimum absorbance reached at the end of each photobleaching process increases, indicating that the destroyed molecules are slightly absorbing white light.

To study the influence of different system parameters, in two similar experiments the switching UV-light power was set to 3.2 nW and 7 nW, respectively. The UV pulse duration was 100 ms and the molecules were photobleached in each cycle with white light for 20 s. In both measurements we have switched in each cycle the vast majority of molecules to the coloured state and back. With the lower UV power of 3.2 nW the absorbance decreased to 50 % after 41 cycles (Fig. 7(a)), i.e. $Z_{50}(3.2 \text{ nW}) = 41$, and with 7 nW we obtain $Z_{50}(7 \text{ nW}) = 20$ (Fig. 7(b)). The total UV energy E_{50} to which the molecules were exposed until reaching Z_{50} was very similar in both experiments, see Table 1. This confirms that the molecules are destroyed due to the UV light and not by the switching process itself.

We were able to increase the cyclability to $Z_{50} \approx 300$ by using a more dense surface coverage. The large number of molecules can be considered as a reservoir of molecules where the destroyed molecules are replaced by still switchable molecules. This clearly underlines the fact that the cyclability is a system parameter and not specific to the molecule. The cyclability obtained so far remains behind the values obtained for macroscopic samples of molecules in solution, which can be up to $Z_{50} \sim 10^4$ for spiropyrans [13,26]. A reason for the lower cyclability using OMFs might for example be the oxygen-containing atmosphere causing light-induced oxidation [27,28].

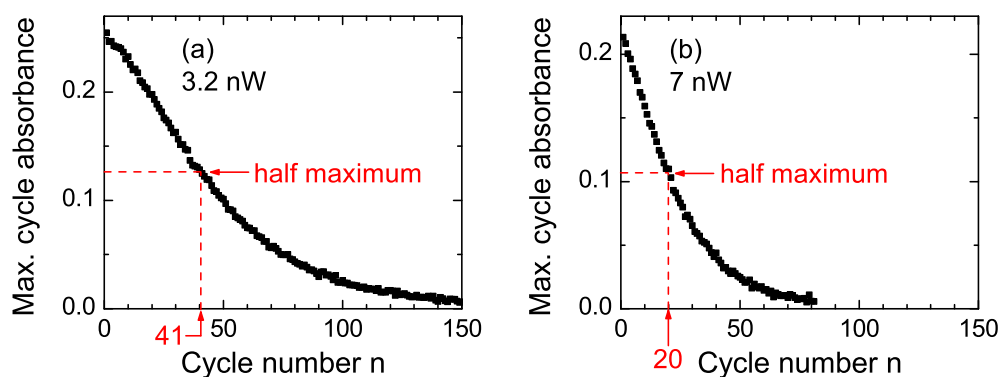


Fig. 7. The maximum cycle absorbance for many subsequent cycles with photocoloration due to the exposure to 3.2 nW (a) and 7 nW (b) of UV light for 100 ms.

Table 1. Cyclability Z_{50} and energy E_{50} .

UV power (nW)	Z_{50}	E_{50} (nJ)
3.2	41	13.1
7	20	14

4.2. Photodestruction quantum yield

The fatigue characteristics of specific photochromic molecules can be characterized by the photodestruction quantum yields ($\Phi_{\text{destr,col}}$, $\Phi_{\text{destr,tr}}$) of the two molecular states. To quantify

$\Phi_{\text{destr,col}}$ of spiroOH we prepare the molecules in the transparent state and then expose them continuously to UV light, see Fig. 8. The initial rise of the absorbance depends on the absorption cross section $\sigma_{\text{tr}}(\text{UV})$ of the transparent molecules at $\lambda = 365$ nm, the UV-light intensity and the switching quantum yield Φ_{photocol} of the transparent molecules. When the photostationary state is reached the absorbance should be stable. However, Fig. 8 shows that the absorbance slowly decreases after the maximum absorbance level is reached. This can be attributed to the fatigue of the molecules, i.e. switchable molecules are destroyed. In the photostationary state we assume that the vast majority of molecules are in the coloured state and therefore attribute the observable photodestruction exclusively to the coloured molecules. The contribution due to white-light absorption of the by-products is below 10 % (see Fig. 6) and is therefore neglected for the following estimation. We thus obtain the ratio of the photocoloration sensitivity $\sigma_{\text{tr}}(\text{UV}) \cdot \Phi_{\text{photocol}}$ to the photodestruction sensitivity $\sigma_{\text{col}}(\text{UV}) \cdot \Phi_{\text{destr,col}}$ by determining the slope of the photocoloration process right after starting the UV exposure and the slope of the absorbance decrease in the photostationary state from Fig. 8

$$\frac{\sigma_{\text{tr}}(\text{UV}) \cdot \Phi_{\text{photocol}}}{\sigma_{\text{col}}(\text{UV}) \cdot \Phi_{\text{destr,col}}} \approx -\frac{\left(\frac{dA}{dt}\right)_{\text{photocol}}}{\left(\frac{dA}{dt}\right)_{\text{destr}}} \approx 500 \quad (7)$$

where $\sigma_{\text{col}}(\text{UV})$ is the absorption cross section of the coloured molecules at $\lambda = 365$ nm. In contrast to the photodestruction, the photocoloration quantum yield is known for many molecules. Therefore, this method can be used to determine the quantum yield of the destructive side reactions of the coloured molecules.

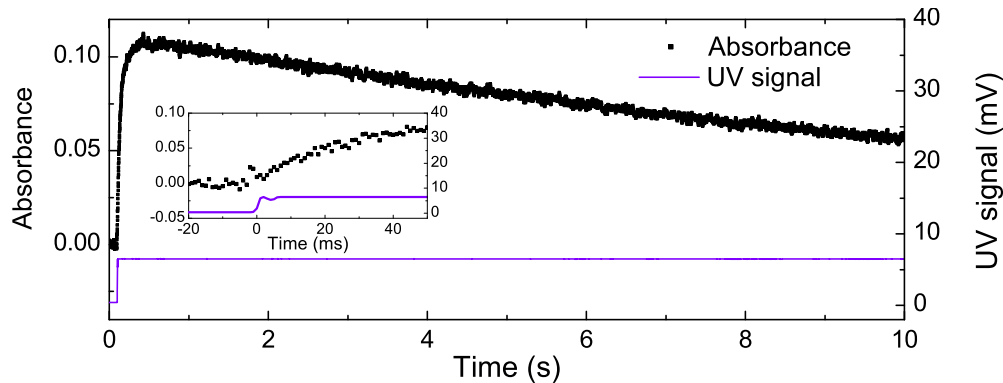


Fig. 8. Fast photocoloration and slow photodestruction of spiroOH under continuous UV exposure (3 nW) used for the determination of the respective sensitivities. The inset shows the horizontally zoomed photocoloration process.

5. Conclusion and outlook

We have presented a new system consisting of photochromic molecules adsorbed on an OMF which can be used to study photochromic processes. We have successfully transferred the functionality which is typically known from macroscopic diluted samples to the microfibre environment. This fibre-based method is an alternative approach to comparable experiments using photochromic molecules in solution (e.g. [15]) or spin-coated samples with different substrates (e.g. [16]). The system has indeed nanoscale properties: minute light powers at the nanowatt level are sufficient to switch molecules between conformational states, but at the same time cause photodestruction already.

The present performance of our system in terms of cyclability and switching speed is not limited by the properties of the individual molecules. Experiments with photochromic molecules in solution show much higher cyclabilities. The fatigue resistance in our experiments can be enhanced by changing the environment such as excluding oxygen by placing the OMFs in a noble gas atmosphere or protecting the molecules by a polymer matrix. State-controlled deposition could increase the number of molecules participating in the switching process. The switching speed can be increased by orders of magnitude by applying tailored laser pulses. Since the switching process of diarylethene molecules themselves occurs on a picosecond timescale (in solution) [22], we expect the dynamics of adsorbed molecules to be governed by a similar time scale. A further improvement of the experimental results can be achieved by reducing the light-molecule coupling inhomogeneities, e.g. at the taper sections.

For characterization and comparison of switchable molecules it would be very useful to define an intrinsic cyclability of the molecules, independent of the optical system. This “ideal cyclability” would specify how often on average a single molecule could be switched before it undergoes a destructive side reaction. As the photodestruction is only caused by the UV light, the critical switching step is the photocolouration. An upper limit to the ideal cyclability can thus be obtained by measuring the ratio of the UV-induced photocolouration and photodestruction quantum yields of the transparent molecules ($Z_{50,ideal} = \Phi_{photocol} / \Phi_{destr,tr}$). To measure $\Phi_{destr,tr}$ instead of $\Phi_{destr,col}$ the measurement in Sec. 4.2 can be modified such that most molecules stay in the transparent state by using e.g. reduced UV power.

Acknowledgments

Financial support by the EC (STREP “CHIMONO”) and the DFG (Research Unit 557) is gratefully acknowledged. We would also like to thank C. Dan for his contribution in the early stages of the experiments and R. Herges, K. Meerholz, and E. Maibach for valuable discussions.